Journal of Pharmacological Sciences 131 (2016) 141–145

Contents lists available at ScienceDirect

Journal of Pharmacological Sciences

journal homepage: www.elsevier.com/locate/jphs

Short communication

A distribution analysis of action potential parameters obtained from patch-clamped human stem cell-derived cardiomyocytes

Fernando López-Redondo [a, **], Junko Kurokawa [b, *], Fumimasa Nomura [a], Tomoyuki Kaneko [c], Tomoyo Hamada [a], Tetsushi Furukawa [b], Kenji Yasuda [a]

[a] Department of Biomedical Information, Institute of Biomaterials and Bioengineering, Tokyo Medical and Dental University, Tokyo, 101-0062, Japan
[b] Department of Bio-informational Pharmacology, Medical Research Institute, Tokyo Medical and Dental University, Tokyo, 113-8510, Japan
[c] Department of Frontier Bioscience, Hosei University, Koganei, Tokyo, 184-8584, Japan

ARTICLE INFO

Article history:
Received 11 December 2015
Received in revised form
3 April 2016
Accepted 10 April 2016
Available online 21 April 2016

Keywords:
iPS cells
Cardiomyocyte
Patch-clamp

ABSTRACT

We investigated electrophysiological properties of human induced-pluripotent-stem-cell-derived and embryonic-stem-cell-derived cardiomyocytes, and analyzed action potential parameters by plotting their frequency distributions. In the both cell lines, the distribution analysis revealed that histograms of maximum upstroke velocity showed two subpopulations with similar intersection values. Sub-populations with faster maximum upstroke velocity showed significant prolongation of action potential durations by application of E-4031, whereas others did not, which may be partly due to shallower maximum diastolic potentials. We described electrophysiological and pharmacological properties of stem-cell-derived cardiomyocytes in the respective sub-populations, which provides a way to characterize diverse electrical properties of stem-cell-derived cardiomyocytes systematically.

Considerable attention has been paid to the potential of human induced pluripotent stem cells (hiPSC) as an unlimited cell source for *in vitro* screening assays, because the production of hiPSC production possess less legal and ethical issues than that of human embryonic stem cells (hESC) (1–3). As a conventional assay for toxicological/pharmacological evaluations, field potentials measurement from multi-cellular preparations with micro-electrode array (MEA) platform (4,5) is utilized to reduce cell-to-cell variation of action potential (AP) dynamics (2,6,7), some reports revealed that considerable variation exists in commercially available cell-lines (8,9). Indeed, mixture of non-myocyte or different types changes excitability of multicellular preparations (10). This indicates necessity of precise information on cell-to-cell variation to understand mechanistic insights on results with conventional MEA assay. However, in previous single-cell analysis, cells were classified into arbitrary three types (i.e. nodal, atrial and ventricular) without applying distribution analysis (6,7,11), mainly because of small cell numbers. Thus, we collected significant numbers of action potential data from patch-clamped hSC-CMs, and analyzed frequency distribution of AP parameters to characterize the cell properties in respective sub-populations.

Cell cultures and isolation of the both cardiomyocytes were performed according to the company's protocols. In brief, frozen hiPSC-CMs (iCell cardiomyocytes, lot#1131800, #1791676, #1341341, iPS PORTAL, Kyoto, Japan) were thawed, and embryoid bodies of hESC-CMs (SA002, Cellartis AB, Gotebörg, Sweden) were shipped. Then, cells were isolated by trypsinization (0.25% trypsin-EDTA) from cell sheets or embryoid bodies respectively, and plated onto 0.5% gelatin/10 μg/ml laminin-coated plasma-etched glass bottom dishes, and used within two weeks. Isolated hiPSC-CMs were maintained in the CDI maintenance medium at 37 °C and at 7% CO_2. Isolated hES-derived cardiomyocytes were maintained in DMEM supplemented with 5 mM GlutaMax™, 20% FBS, 1% Pen/Strep, 1% non-essential amino acids, 0.2% 2-mercaptoethanol, and were kept at 37 °C and 5% CO_2. E-4031 (4′-[[1-[2-(6-methyl-2-pyridyl)ethyl]-4-piperidinyl]carboxyl]methanesulfonanilide dihydrochloride dehydrate, Eisai Co., Tokyo) was kept as 10 mM stock in

* Corresponding author. 1-5-45 Yushima, Bunkyo-ku, Tokyo, 113-8510, Japan. Tel.: +81 3 5803 4951; fax: +81 3 5803 0364.
** Corresponding author. Division of Genomic Technologies, RIKEN Center of Life Science Technologies, Yokohama, 230-0045, Japan.
E-mail addresses: fernando.lopezredondo@riken.jp (F. López-Redondo), junkokuro.bip@mri.tmd.ac.jp (J. Kurokawa).

Peer review under responsibility of Japanese Pharmacological Society.

http://dx.doi.org/10.1016/j.jphs.2016.04.015

distilled water. All other materials were reagent quality and obtained from standard sources.

Action potentials were recorded at 36 ± 1 °C with the perforated patch configuration as described previously (12). External solution contained (in mM): NaCl (135), NaH_2PO_4 (0.33), KCl (5.4), $CaCl_2$ (1.8), $MgCl_2$ (0.53), glucose (5.5), HEPES (5), pH 7.4. To achieve patch perforation (<20 MΩ; series resistances), amphotericin B (0.3 μg/ml) was added to the internal solution composed of (in mM): potassium-aspartate (110), KCl (30), $CaCl_2$ (1), adenosine-5′-triphosphate magnesium salt (5), creatine phosphate disodium salt (5), HEPES (5), EGTA (11), pH 7.25. We adopted the AP data only when more than 35 stable AP traces were recorded. Data were acquired and analyzed using pClamp10 software (Molecular Devices, Sunnyvale, CA, USA). In quiescent cells, 2-ms duration current pulses (120% of the threshold intensity) were applied to elicit APs. All values are presented as mean ± S.E.M. Statistical significance was assessed with Student's *t*-test for simple comparisons and non-parametric Kolmogorov–Smirnov test for frequency distributions by using OriginPro 8 software (Origin Lab Co, Northampton MA, USA). Differences at $P < 0.05$ were considered to be significant.

In Fig. 1 and Table 1, APs recorded from 54 hiPSC-CMs and 80 hESC-CMs were summarized. Although the beating rate (BR) in hiPSC-CMs was significantly slower than that in hESC-CMs with comparing two averages (Table 1), it is difficult to conclude that these cells have different phenotypes. Because the distribution analysis revealed that hiPS-CM in itself would have at least more than two phenotypes, which is consistent with significantly larger variations of beat-to-beat times shown as bigger coefficient of variation (CV) in hiPS-CM (Fig. 1A and Table 1).

In terms of AP parameters, there was no statistical difference in average values of AP parameters (Table 1): AP amplitude (APA), AP duration at 50% and 70% of repolarization (APD_{50}, APD_{70}), maximum upstroke velocity (dV/dt_{max}), APD ratio during phase 2 (APD_{20-40}/APD_{50-70}); an indicative of AP plateau, and APD ratio (APD_{90}/APD_{50}); an indicative of phase 4 depolarization, except of slight but significant differences in mean values of maximum diastolic potential (MDP) (Table 1). Relatively large

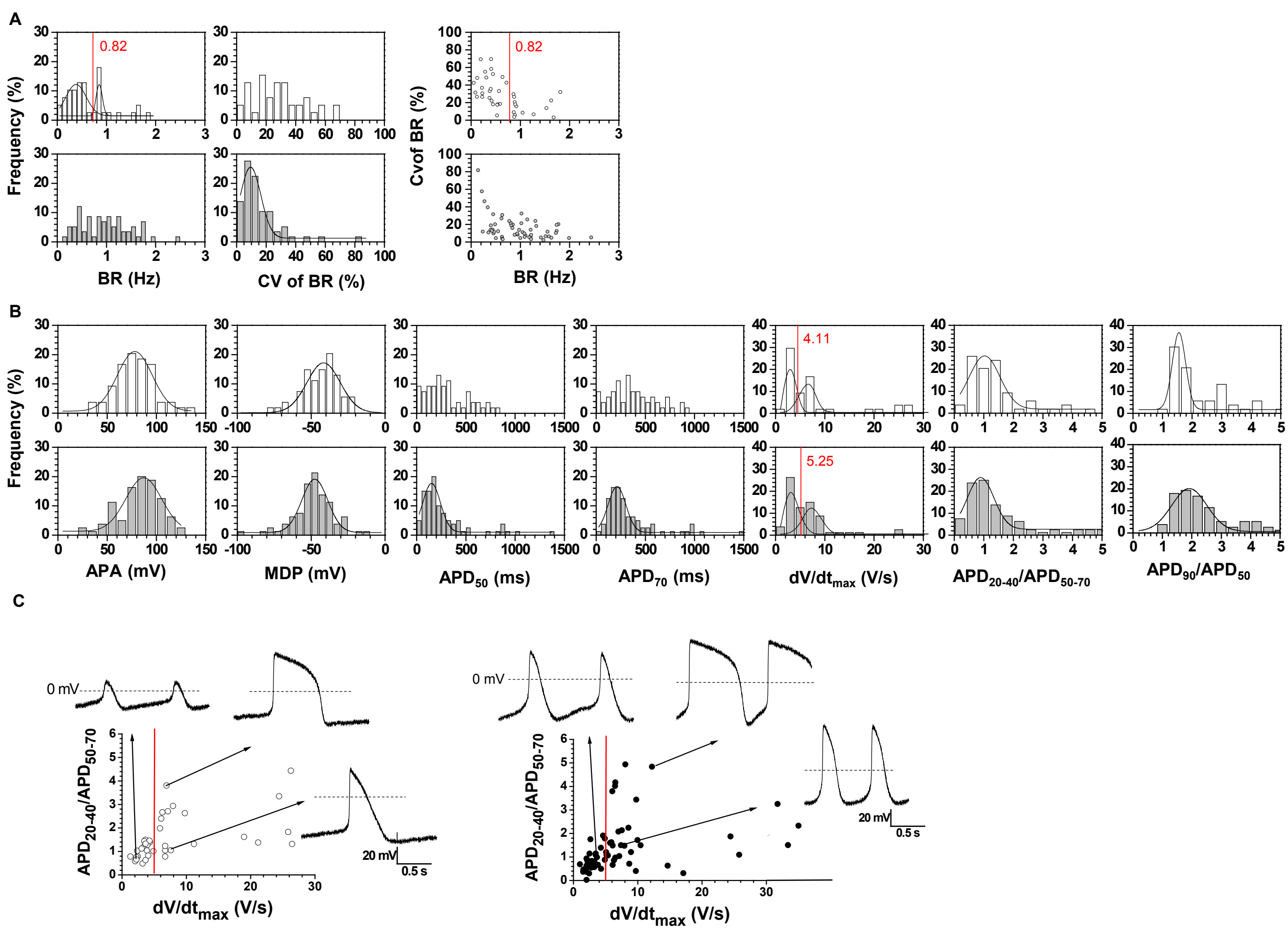

Fig. 1. Distributions of electrophysiological parameters in hiPSC- and hESC-derived cardiomyocytes (CMs). Histograms for AP (**A**) and beating rate (**B**) parameters were fitted with single or multiple Gaussian distributions. Multiple Gaussian functions were applied when coefficient of determination (R^2) on single Gaussian fitting fell below 0.81. Rate (%) of each fraction (i.e. peak) in multiple fitting was calculated from ratio of each peak area. **(A)** Frequency distribution of BR and its coefficient of variation (CV) in spontaneously AP firing 39 hiPSC-CMs (white bars, upper panels) and 54 hESC-CMs (gray bars, lower panels). The distribution on the BR of hiPSC-CMs showed two major peaks at 0.38 Hz (69.8%) and 0.88 Hz (30.2%) of Gaussian distribution (intersection 0.82 Hz, $R^2 = 0.88$). **(B)** Frequency distribution of AP parameters in 54 hiPSC-CMs (white bars, upper panels) and 80 hESC-CMs (gray bars, lower panels). Frequency peaks (% fraction for multiple distributions) of dV/dt_{max} are as follows: hiPSC-CMs; 2.6 V/s (50.8%) and 6.4 V/s (49.2%) (intersection 4.11 V/s, $R^2 = 0.927$), and hESC-CMs; 3.3 V/s (50.8%) and 7.4 V/s (49.2%) on hESC-CMs (intersection 5.25 V/s, $R^2 = 0.941$), respectively. The intersections of bimodal distributions for dV/dt_{max} were shown in red dotted lines. **(C)** Scatterplot representation of upstroke velocity (dV/dt_{max}) against APD_{20-40}/APD_{50-70} ratio in hiPSC-CMs (white dots, left panel) and hESC-CMs (black dots, right panel). Representative AP waveforms at precincts are shown in insets.

Table 1
Summary of action potential parameters obtained from individual hiPS-cardiomyocytes and hES-cardiomyocytes. Action potential (AP) parameters (mean ± S.E.M.) were determined by averaging data from three consecutive APs at steady state. * $P < 0.05$, ** $P < 0.01$, *** $P < 0.001$ unpaired Student's *t*-test.

Spontaneous and paced AP	hiPS-CMs (n = 54)	hES-CMs (n = 80)
APA (mV)	79.4 ± 2.9	81.8 ± 2.5
MDP (mV)	−43.3 ± 1.7	−48.9 ± 1.5*
APD50 (ms)	309.4 ± 29.5	273.7 ± 28.7
APD70 (ms)	380.0 ± 32.2	339.4 ± 30.1
APD20−40/APD50−70	1.4 ± 0.1	1.5 ± 0.1
APD90/APD50	2.8 ± 0.3	2.9 ± 0.2
dV/dtmax	27.3 ± 5.3	18.0 ± 2.6
Spontaneous AP only	**hiPS-CMs (n = 39; 72% out of total cell numbers)**	**hES-CMs (n = 58; 73% out of total cell numbers)**
Beating rate (Hz)	0.6 ± 0.1	1.0 ± 0.1**
CV of beating rate (%)	28.9 ± 2.8	15.9 ± 1.9***

APA: action potential amplitude, CM: cardiomyocytes, MDP: maximum diastolic potential, APD_{50} and APD_{70}: action potential duration at 50 and 70% of repolarization, dV/dt_{max}: maximum upstroke velocity, APD_{20}−APD_{40}/APD_{50}−APD_{70}: APD ratio which indicates "plateau" during phase 2, APD_{90}/APD_{50}: APD ratio which indicates the presence of phase 4 depolarization, CV: coefficient of variation indicating SD/mean.

S.E.M. values for AP parameters reminded us that the data distributed in a wide range. We therefore plotted the data with frequency distribution. In Fig. 1A and B, the histogram for most of parameters was fitted to single Gaussian distributions with more than 0.81 of R^2 values (Fig. 1B). Exceptionally, histograms on APD_{50} and APD_{70} of hiPSC-CMs were widely distributed, and R^2 values of the fitting could not be less than 0.81 using multiple Gaussian fitting, or not be converged to the single result. Despite differences on each APD parameter, mean values for ratios of APD (APD_{20-40}/APD_{50-70} and APD_{90}/APD_{50}) were similar and were fitted with single Gaussian distribution in both cell-lines (Table 1 and Fig. 1B), indicating indistinguishable at repolarization processes. On the other hand, the histograms of dV/dt_{max}, upstroke velocity, showed bimodal distributions composed of a slow and a fast fraction. In these cases, intersections of two Gaussian curves in hiPSC-CMS and hESC-CMs were 4.11 (V/s) and 5.25 (V/s), respectively. Although these subtle differences existed in the distribution pattern, there was no statistical significance for differences of AP parameters between hiPSC-CMs and hESC-CMs as previously described by others (13). Fig. 1C shows the relationship between waveform of action potential and two AP parameters. These parameters (APD_{20-40}/APD_{50-70} and dV/dt_{max}) are well-known indices reflecting the duration of depolarization or plateau phase, so it is usable to distinguish the cell types, i.e., between nodal and atrial/ventricular types, or between atrial and ventricular types. When APD_{20-40}/APD_{50-70} was plotted against dV/dt_{max} in Fig. 1C, arbitrary "ventricular-like" cells were seen only if dV/dt_{max} was larger than 4.11 (V/s) on hiPSC-CMs and 5.25 (V/s) in hESC-CMs, respectively. Additional distribution analysis with faster dV/dt_{max} in Supplementary Figure 1 did not provide numerical criteria to segregate "atrial-like" and "ventricular-like".

In Fig. 2, the effects of a standard hERG blocker, E-4031, on AP traces were investigated both in hiPSC-CMs and hESC-CMs. According to previous reports on cardiac toxicological assessment using hSC-CMs, it has been noticed that "ventricular-like" cells are more responsive to QT-prolonging drugs (6), but no study has provided any numerical criteria of AP parameters to categorize "ventricular-like" cells. We therefore asked whether our distribution analysis allows segregating cell populations which are responsive to drugs. To test this, we employed the intersection dV/dt_{max} values (4.11 V/s for hiPS-CMs and 5.25 V/s for hES-CMs) (Fig. 1B). Then, the effect of E-4031 on APD was investigated in two subpopulations with slow or fast dV/dt_{max} (Fig. 2D). Without considering the subpopulations, we found a wide variety of responses to E4031 application at each concentration tested, resulting in neither evident effect on APD_{70} nor occurrence of EAD (Fig. 2A–C). With considering the subpopulations in Fig. 2D and F, in the case of hiPSC-CMs with fast upstroke velocity (7 cells), E-4031 at 10 nM tended to prolong APD_{70}, although it was not statistically significant ($P = 0.08$). In these cells, high concentration of E-4031 did not alter APD_{70}, which is due to dramatic AP alternation as shown in Fig. 2B right. In contrast, in the case of hiPSC-CMs with slow upstroke velocity (3 cells), E-4031 either at 10 nM and 100 nM did not alter APD_{70} (2 out of 3 cells) or arrested (1 out of 3 cells). Similar results were obtained in hESC-CMs. With fast upstroke velocity (9 cells), E-4031 at 10 nM tended to prolong APD_{70} but not significantly ($P = 0.05$), and an application of 100 nM E-4031 (4 out of 9 cells) diminished the tendency. With slow upstroke velocity (3 cells), the E-4031 application did not alter APD_{70} and arrested at 100 nM in one out of 3 cells. E4031 also depolarized MDP in some cells (Fig. 2A). But there was no significant effect on MDP, when all the data were analyzed (Fig. 2E). In the hiPSC-CMs, the subpopulation with slow upstroke velocity had shallower MDP than that with fast upstroke velocity. But effects of E-4031 on MDP were unclear (Fig. 2F). In hESC-CMs, the difference of MDP without drugs between slow or fast upstroke velocities was not clear as shown in hiPSC-cardiomyocytes (Fig. 2F).

In this study, we evaluated basic electrophysiological characteristics of hiPSC-CMs, and they were compared with those of hESC-CMs by analyzing frequency distribution. The major findings of this study are as follows: (1) Average values of the AP parameters in hiPSC-CMs and hESC-CMs were statistically undistinguishable from each other with the exception of MDP and beating rate. (2) Our distribution analysis of AP parameters from single cell data presented a way to set numerical criteria to segregate respective subpopulations. (3) It is possible that the subpopulation with fast upstroke velocity exhibit APD prolongation by an application of E-4031.

If respective subpopulations of hSC-CMs exhibit various pharmacological responses, it may be worth knowing respective cell properties to understand molecular mechanisms for developing specific cell types or predicting multicellular responses by system biological approaches. Although long APD_{90} has been used as an arbitrary criterion for drug sensitivity in a particular cell source (9), it must be difficult to apply this to others (8,13). Our distribution analysis proposed a possible way to set numerical criteria for drug sensitivity, although more cell numbers or higher purity or greater maturation may be necessary in the future. In conclusion, our distribution analysis could add useful information on electrophysiological properties of hiPSC-CMs for *in vitro* pharmacological screening assays.

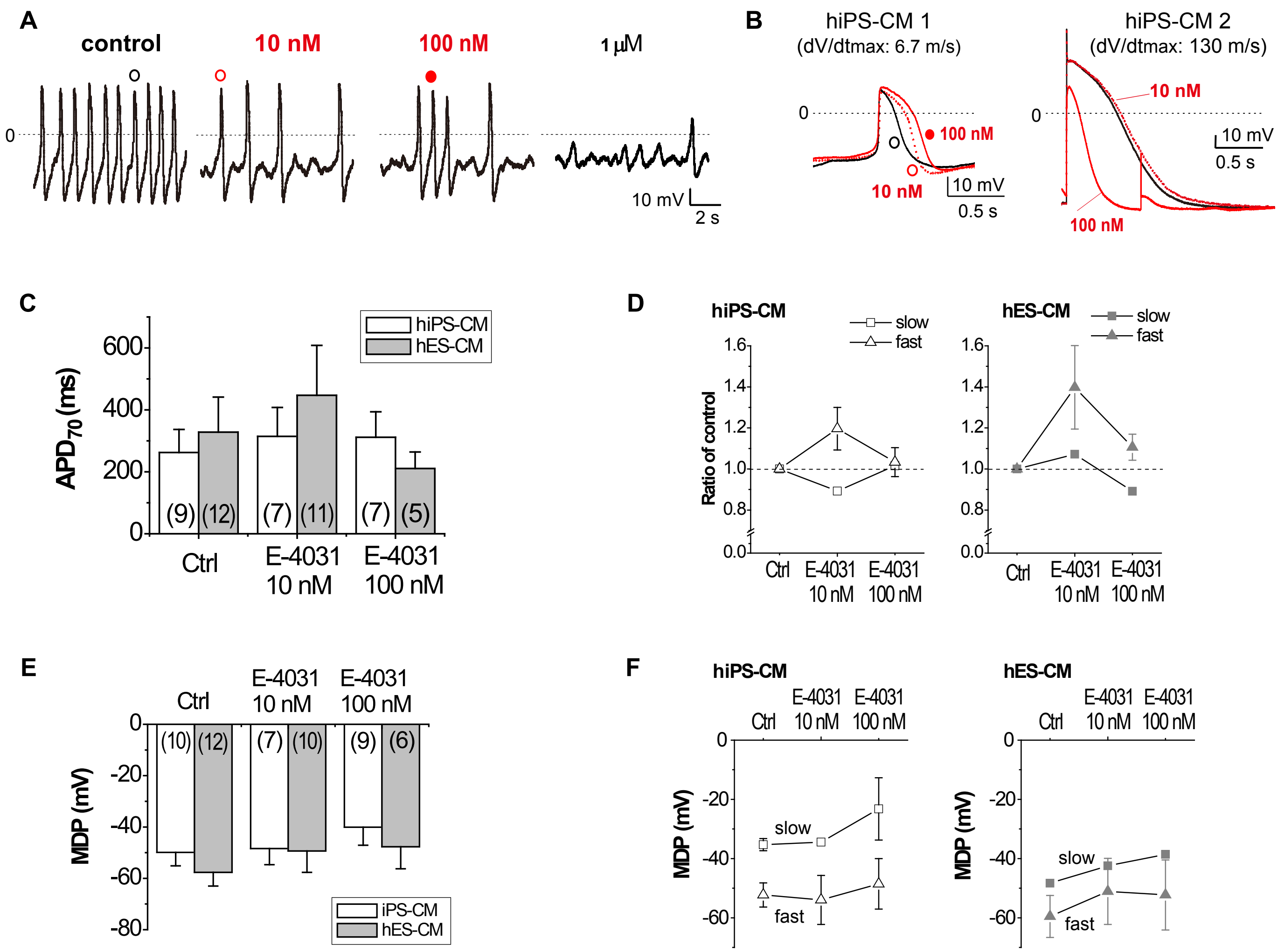

Fig. 2. Effects of E-4031 on APD_{70} in hiPSC-CMs and hESC-CMs. **(A)** Representative AP waveforms in hiPSC-CM 1 (**B**, *left*) without (control) or with E-4031 (10, 100 nM and 1 μM). **(B)** Individual variability in the response to E-4031. Overlay of expanded traces marked in (**A**) with open black dot (control), open red dot (10 nM) and closed red dot (100 nM) (left). hiPSC-CM2 showing decreasing effect on APD_{70} at 100 nM E-4031 (right). **(C)** Dose-response bar graphs of E-4031 effect on APD_{70}. hESC-CMs white bars and hESC-CMs gray bars. **(D)** Effect of E4031 effect on the subpopulations segregated by cut-off points of dV/dt_{max} (4.11 V/s for hiPS-CM, and 5.25 V/s for hES-CMs) resulting from Fig. 1A. Cells with faster upstroke (>4.11 V/s for hiPS-CMs and >5.25 V/s for hES-CMs) presented enhanced prolongation of APD_{70}. **(E)** Bar graph of the depolarizing effect elicited by E-4031. Each bar indicates mean ± SEM. n: indicated by numbers in brackets. No significant differences were found. **(F)** Dose-response curves of E4031 effect on MDP of the two cell subpopulations. Left: hiPSC-CM with slow (white squares) and fast (white triangles) dV/dt_{max}. Right: hESC-CM with slow (gray squares) and fast (gray triangles).

Disclosures

The authors declared no conflict of interest.

Acknowledgments

This research was supported by the Japan New Energy and Industrial Technology Development Organization (NEDO) (P08030). The authors are grateful to Ms. Reiko Osumi, Ms. Reiko Kimura, Ms. Akiko Hagiya, Ms. Tamae Takato and Ms. Naoko Ishii for technical assistance.

Appendix A. Supplementary material

Supplementary data related to this article can be found at http://dx.doi.org/10.1016/j.jphs.2016.04.015.

References

(1) Takahashi K, Tanabe K, Ohnuki M, Narita M, Ichisaka T, Tomoda K, et al. Induction of pluripotent stem cells from adult human fibroblasts by defined factors. Cell. 2007;131:861–872.
(2) Mummery C, Ward-van Oostwaard D, Doevendans P, Spijker R, van den Brink S, Hassink R, et al. Differentiation of human embryonic stem cells to cardiomyocytes: role of coculture with visceral endoderm-like cells. Circulation. 2003;107:2733–2740.
(3) Chi KR. Revolution dawning in cardiotoxicity testing. Nat Rev Drug Discov. 2013;12:565–567.
(4) Fermini B, Hancox JC, Abi-Gerges N, Bridgland-Taylor M, Chaudhary KW, Colatsky T, et al. A new perspective in the field of cardiac safety testing through the comprehensive in vitro proarrhythmia assay paradigm. J Biomol Screen. 2016;21:1–11.
(5) Nakamura Y, Matsuo J, Miyamoto N, Ojima A, Ando K, Kanda Y, et al. Assessment of testing methods for drug-induced repolarization delay and arrhythmias in an iPS cell-derived cardiomyocyte sheet: multi-site validation study. J Pharmacol Sci. 2014;124:494–501.
(6) Gibson JK, Yue Y, Bronson J, Palmer C, Numann R. Human stem cell-derived cardiomyocytes detect drug-mediated changes in action potentials and ion currents. J Pharmacol Toxicol Methods. 2014;70:255–267.
(7) He JQ, Ma Y, Lee Y, Thomson JA, Kamp TJ. Human embryonic stem cells develop into multiple types of cardiac myocytes: action potential characterization. Circ Res. 2003;93:32–39.

(8) Cavero I, Holzgrefe H. CiPA: ongoing testing, future qualification procedures, and pending issues. J Pharmacol Toxicol Methods. 2015;76:27–37.
(9) Jonsson MKB, Duker G, Tropp C, Andersson B, Sartipy P, Vos MA, et al. Quantified proarrhythmic potential of selected human embryonic stem cell-derived cardiomyocytes. Stem Cell Res. 2010;4:189–200.
(10) Kaneko T, Nomura F, Yasuda K. On-chip constructive cell-network study (I): contribution of cardiac fibroblasts to cardiomyocyte beating synchronization and community effect. J Nanobiotechnol. 2011;9:21–33.
(11) Ma J, Guo L, Fiene SJ, Anson BD, Thomson JA, Kamp TJ, et al. High purity human-induced pluripotent stem cell-derived cardiomyocytes: electrophysiological properties of action potentials and ionic currents. Am J Physiol Heart Circ Physiol. 2011;301:H2006–H2017.
(12) Kurokawa J, Tamagawa M, Harada N, Honda S, Bai CX, Nakaya H, et al. Acute effects of oestrogen on the guinea pig and human ikr channels and drug-induced prolongation of cardiac repolarization. J Physiol. 2008;586:2961–2973.
(13) Gupta MK, Illich DJ, Gaarz A, Matzkies M, Nguemo F, Pfannkuche K, et al. Global transcriptional profiles of beating clusters derived from human induced pluripotent stem cells and embryonic stem cells are highly similar. BMC Dev Biol. 2010;10:98.